Nonlinear Effects from Dipolar Interactions in Hyperpolarized Liquid ^{129}Xe

M. P. Ledbetter and M. V. Romalis

Department of Physics, Princeton University, Princeton, New Jersey 08544

(Received 4 July 2002; published 30 December 2002)

We investigate nonlinear effects of long-range dipolar interactions in a spherical sample of hyperpolarized liquid ^{129}Xe. Using two high-T_c SQUID detectors we directly measure the evolution of the magnetization gradients. For small initial rf tip angles we observe an increase in the transverse relaxation time T_2^* by a factor of 5 and coherent oscillations of magnetization gradients. For large tip angles we observe an exponential growth of the magnetization gradients and demonstrate a gain in sensitivity to magnetic field gradients by a factor of 10. Our results are in quantitative agreement with simple analytical predictions. We discuss applications of these nonlinear effects for precision measurements.

DOI: 10.1103/PhysRevLett.89.287601 PACS numbers: 76.60.Jx, 05.45.–a, 33.25.+k

In liquid state NMR the magnetic dipolar interactions between neighboring spins quickly average out due to diffusion, yielding very narrow NMR lines. However, dipolar fields from distant spins do not average out and can lead to dramatic effects if the average magnetization of the sample is sufficiently large. Such nonlinear effects due to long-range dipolar interactions have recently attracted much attention [1–6]. While they often represent a nuisance for high resolution NMR, they can also be used to enhance sensitivity in precision measurements, for example, in a search for a permanent electric dipole moment (EDM) in liquid ^{129}Xe [7]. Long-range dipolar interactions in cold gases have also generated much interest recently [8]. Under certain conditions long-range dipolar interactions lead to an instability of a uniform magnetization distribution such that any perturbation produces exponentially growing magnetization gradients. Previous experimental investigations of these effects used conventional NMR techniques and focused on the behavior of free induction decay (FID) signals [2–5] or spin-echo trains [7] that are sensitive only to the total magnetization of the sample.

Here we describe the results of the first study of nonlinear dipolar effects using two SQUID magnetometers that allow a direct measurement of the magnetization gradients in the sample. The SQUID magnetometers have pickup coils comparable to the size of the sample and are preferentially sensitive to magnetization in different parts of the cell. The phase difference between the signals detected in the two SQUIDs is directly proportional to the first-order gradient of the magnetization.

We observe two distinct regimes in the behavior of the magnetization gradients, in agreement with previous theoretical predictions [1,6]. For small tip angles of the magnetization from the magnetic field the dipolar interactions lead to a suppression of the magnetization dephasing in external field gradients. We observe FIDs that last 5 times longer than would be expected in the absence of dipolar fields. We also observe coherent oscillations of the magnetization gradients in good agreement with simple analytical models. For large tip angles we observe an exponential growth of the magnetization gradients in excellent agreement with predictions. We demonstrate how this exponential growth of the phase difference can be used to obtain an enhancement of sensitivity to magnetic field gradients. Theoretical amplification factors can be extremely large, while experimentally we have observed amplification by more than a factor of 10.

The measurements are performed using hyperpolarized liquid ^{129}Xe in a magnetic field of 10 mG. Such low-field environment is particularly well suited for precision measurements. We obtain ambient magnetic field gradients of about 1 μG/cm without using shimming coils. By using a hyperpolarized liquid and SQUID magnetometers sensitive to dc flux we completely avoid the usual penalty in signal-to-noise ratio associated with low-field NMR.

Hyperpolarized ^{129}Xe is produced using the standard method of spin-exchange optical pumping [7,9]. The gas flows through an optical pumping cell where it is polarized by spin exchange with Rb vapor. Polarized ^{129}Xe (in natural abundance) is accumulated in ice form at 77 K in a 2 kG magnetic field. After approximately 25 min the ice is melted and the gas flows through a 1/4 in. copper tube into the magnetic shields and condenses in a spherical glass cell with an inner radius $R = 0.617 \pm 0.005$ cm, as shown in Fig. 1. A set of coils inside the shields creates a 10 mG magnetic field and allows application of rf pulses with a true rotating field and control of linear magnetic field gradients. The NMR signal is detected using high-T_c SQUID detectors made by Tristan Technologies [10]. The pickup coil of the SQUID detectors is an 8×8 mm square loop. They are located 1.6 cm from the center of the cell and are tilted by 45° relative to the magnetic field. To accurately determine the position of the SQUIDs relative to the Xe cell we attach a calibration wire loop to the cell and measure the size of the signal that a small current flowing through the loop induces in the SQUIDs. We image the cell onto a CCD camera to monitor the collection of liquid Xe. By combining this information

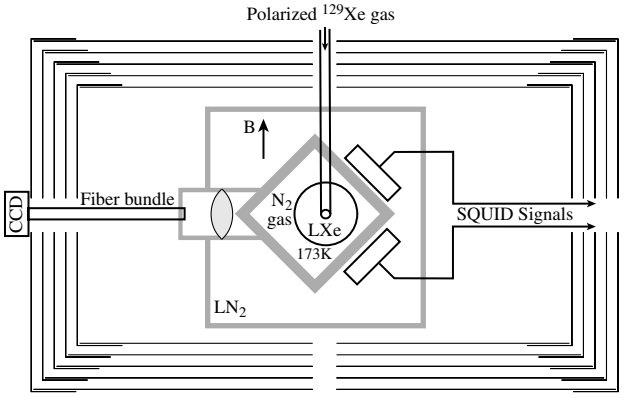

FIG. 1. Low field NMR setup (view from above). Polarized liquid ^{129}Xe is contained in a spherical cell maintained at 173 K by flowing N_2 gas. High-T_c SQUIDs are submerged in LN_2. The Dewar is made from G11 fiberglass.

with the buildup of dc magnetization detected by the SQUIDs we can monitor the uniformity of the polarization of ^{129}Xe as it condenses in the cell.

Most of the features of our data can be understood using a simple model for magnetization gradient growth discussed in [7] extended to arbitrary tip angles. Here we limit the discussion to the effects of longitudinal field gradients, $\mathbf{H} = (H_0 + gz)\hat{\mathbf{z}}$. We first consider an expansion of the magnetization keeping only linear gradients in the direction of the applied gradient,

$$\mathbf{M}(\mathbf{r}, t) = \mathbf{M}_0 + \mathbf{m}(t) M_0 \frac{z}{R}, \tag{1}$$

and later consider the effects of higher-order terms. In a spherical cell linear magnetization gradients create only linear gradients of dipolar fields. In the rotating frame, the total magnetic field is

$$\mathbf{B} = \left\{ \frac{8\pi M_0 z}{15R} m_x, \frac{8\pi M_0 z}{15R} m_y, -\frac{16\pi M_0 z}{15R} m_z + gz \right\}. \tag{2}$$

The time evolution of the magnetization is determined using the Bloch equations $d\mathbf{M}/dt = \gamma \mathbf{M} \times \mathbf{B}$. Spin relaxation [7] and diffusion [11] can be neglected, as their time scales are much longer than the time scale for dipolar interactions. We assume an initial uniform magnetization M_0 along the $\hat{z}$ axis and consider the evolution after an rf pulse that tips it by an angle α into the $\hat{x}$ direction of the rotating frame. While all components of the magnetization develop some gradients, our measurements are primarily sensitive to the gradient of the $\hat{y}$ component. Substituting Eqs. (1) and (2) into the Bloch equations gives the following time evolution for the dimensionless linear magnetization gradient parameter m_y:

$$m_y(t) = -\frac{\gamma g R}{\beta} \sin(\alpha) \sinh(\beta t), \tag{3}$$

$$\beta = \frac{4\sqrt{2}\pi}{15} M_0 \gamma (1 - 3\cos(2\alpha))^{1/2}. \tag{4}$$

Here β is proportional to the strength of the long-range dipolar interactions. The magnetization gradient parameter m_y can be directly measured as a phase difference $\Delta\phi$ between the ac signals detected in the two SQUIDs, as illustrated in the inset of Fig. 2. We calculate the convolution of the spatial magnetic field sensitivity of the SQUIDs with the magnetization profile and find that for $m_y \lesssim 1$ the phase difference $\Delta\phi = \zeta m_y / \sin(\alpha)$, where ζ is a numerical factor that depends on geometry, for our dimensions $\zeta = 0.46 \pm 0.01$.

From Eq. (4) it immediately follows that for $\alpha > 35°$ (real β) the dipolar interactions lead to exponential growth of magnetization gradients, while for $\alpha < 35°$ (imaginary β) they produce oscillating magnetization gradients. Exponential dephasing for $\alpha > 35°$ was first predicted in [1] based on a numerical model. It has been observed indirectly as a sharp drop in the amplitude of an FID [4] or a spin-echo train [7]. Using two independent detectors we directly measure the initial evolution of the magnetization gradients before they lead to an appreciable change in the overall size of the NMR signal. The top panel of Fig. 2 shows the signals from the two SQUIDS following a 90° pulse in the presence of a linear magnetic field gradient $g = 8.4 \pm 1.0$ μG/cm. The circles in the bottom panel show the phase difference between the two signals.

We determine the initial magnetization from the amplitude of the SQUID signals. For this data set

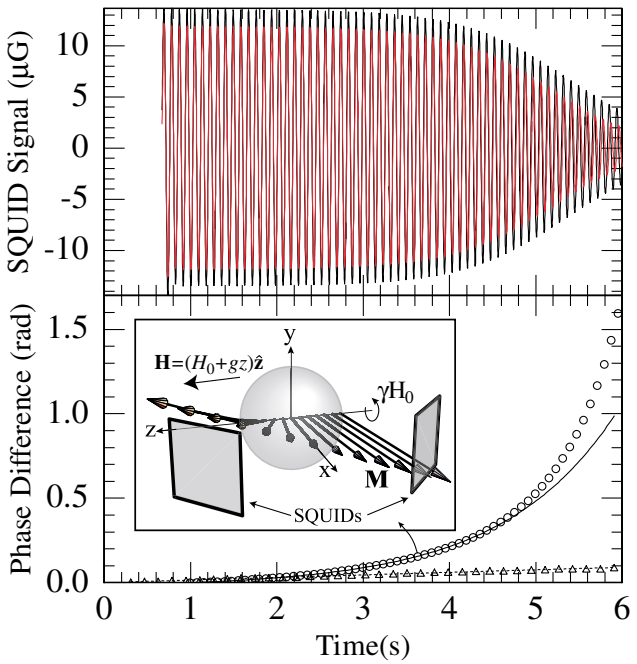

FIG. 2 (color online). SQUID signals (top plot) and the phase difference between them (bottom plot, circles) following a 90° pulse. The initial phase evolution ($t < 4.5$ sec) is well described by a fit based on Eq. (3) (solid line). Inset: Relative orientation of the magnetization and SQUIDs at $t = 3.6$ s. Triangles show data with the same field gradient but a 35° pulse together with a linear fit (dashed line) based on Eq. (5).

$M_0 = 42 \pm 2$ μG where the error is dominated by the uncertainties in the dimensions of the cell and the distance from the cell to the SQUIDs. From Eq. (4) we obtain $\beta = 0.74 \pm 0.04$ sec^{-1} while a fit to the phase difference data based on Eq. (3) gives $\beta = 0.75$ sec^{-1} and a magnetic field gradient $g = 8.0$ μG/cm. We obtained equally good agreement with the model in other data sets with a wide range of M_0 and g. The phase difference begins to deviate from the predictions of the linear model when $m_y/\sin(\alpha) = \Delta\phi/\zeta$ reaches approximately 0.5.

It also follows from Eq. (4) that for $\alpha = 35°$ the effects of dipolar interactions can be turned off as long as the linear expansion of the magnetization remains valid. For $\beta = 0$ the phase difference grows linearly in time

$$\Delta\phi = \zeta\gamma g R t, \tag{5}$$

as shown by the triangles in the bottom panel of Fig. 2 for $M_0 = 24$ μG. For these data the applied magnetic field gradient is $g = 8.4 \pm 1.0$ μG/cm while the fit to the phase difference gives $g = 7.2$ μG/cm.

For large tip angles the ^{129}Xe atoms act as a self-gradiometer, amplifying the magnetization gradients by a factor $G = \sinh(\beta t)/\beta t$ until they become large. Given a certain noise level in the detection of the phase difference it allows a significant improvement in the sensitivity to small changes of the magnetic field gradient g or a reduction in the measurement time. In Fig. 2 the amplification factor is given by the ratio of the solid and dashed lines and reaches about 10 at $t = 5.5$ sec. The amplification factor G in principle can be extremely large since damping of the magnetization gradients due to diffusion and transverse relaxation occurs on a time scale of hundreds of seconds. Using two SQUID detectors it is possible to measure the phase evolution before there is a substantial decay in the amplitude of the signal and apply a feedback to the magnetic field gradient to prevent dephasing of the spins. By applying a small rotating magnetic field it should also be possible to suppress the dephasing due to transverse magnetic field gradients [7]. Technical limitations such as fluctuations in the magnetization distribution and magnetic field gradients are likely to limit the maximum achievable gain in sensitivity. As discussed in [7] this amplification of magnetic field gradients can be used to increase the sensitivity in an EDM search.

For tip angles α less than 35° Eq. (3) predicts oscillations of the magnetization gradients preventing their linear growth. The behavior of the magnetization for $\alpha = 3.5°$ and a magnetic field gradient $g = 42$ μG/cm is shown in Fig. 3. We indeed observe such oscillations as well as a dramatic increase of the transverse relaxation time. The decay of the transverse signal expected in the absence of dipolar interactions is shown by the dot-dashed line in Fig. 3 and is about 5 times faster than what we measure. This behavior was observed for all data sets with tip angles ranging from 3.5° to 20°, magnetizations from 10 to 80 μG, and external field gradients from 12 to 120 μG/cm. Similar effects of "spectral clustering" have been previously observed in U shaped samples [4,12] where the initial magnetic field inhomogeneities are caused by the magnetization itself. In our case the signals have only one spectral line and dipolar interactions lead to "spectral narrowing" in external field gradients. This effect can in certain cases increase the NMR frequency resolution without the need for careful shimming of the magnetic field gradients.

Several features of our small tip angle data are well described by the model including only linear magnetization gradients. Equation (3) predicts a frequency $\omega_{th} = i\beta$ and an amplitude $A_{th} = \zeta\gamma g R/\omega_{th}$ for the oscillations in the phase difference, but does not explain their decay. We fit the oscillations to an exponentially decaying sine wave $\Delta\phi = A\sin(\omega t)\exp(-t/\tau)$, although the decay is only approximately exponential. Figure 4 shows with circles a comparison of the amplitude and frequency of the oscillations with the predictions of the model for all data sets. We find that the model works well for the amplitude of the oscillations, which reflects the initial rate of gradient growth and for the frequency of oscillations with a small amplitude, when the magnetization gradients are small.

Other qualitative features of our data cannot be accounted for by the simple model. The decay time of the phase oscillations τ, which ranges from 8 to 60 sec, is too fast to be explained by diffusion. We find that $1/\tau$

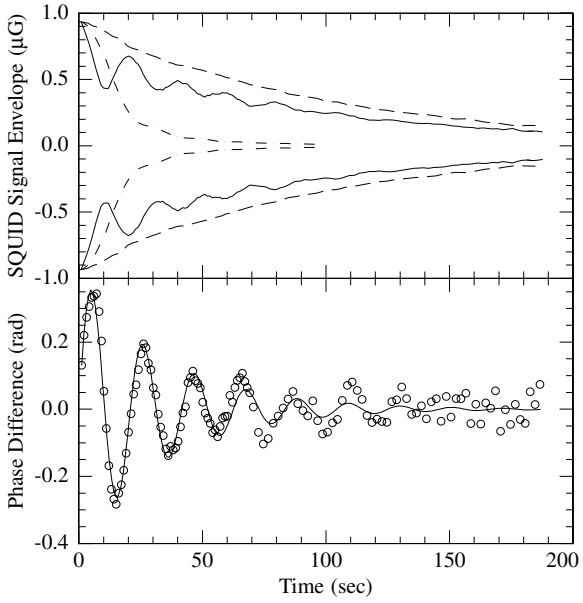

FIG. 3. Top panel: Envelope of the two SQUID signals (solid and dashed lines) following a 3.5° pulse in a 42 μG/cm gradient. In the absence of dipolar interactions much faster decay of the signal (dot-dashed lines) is expected. Bottom panel: Phase difference between the SQUID signals with a fit to exponentially decaying oscillations (solid line).

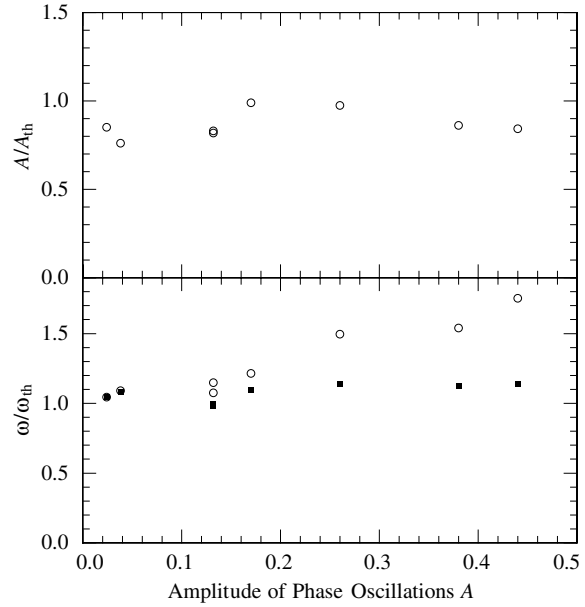

FIG. 4. Ratio of the amplitude (top panel) and frequency (bottom panel, open circles) of the phase oscillations to the predictions of the linear gradient model. Solid squares show the ratio using the model including higher order gradients.

approximately scales with the magnetization and is likely due to higher-order magnetization gradients. Another interesting feature is a dramatic difference in the envelope of the two SQUID signals, shown in Fig. 3. We find that for the SQUID located on the side of the cell where zgM_0 is negative the signal has a pronounced amplitude modulation proportional to the amplitude of the phase oscillations, while on the side where zgM_0 is positive the signal has almost no amplitude modulation. Also note that after the decay of amplitude modulation the signals in the two SQUIDs are slightly different, indicating that the magnetization develops a steady-state gradient.

To account for these features we extend our model by including higher-order terms in the expansion of the magnetization given by Eq. (1). We include all terms of the form $z^n(x^2 + y^2)^m/R^{n+2m}$ with $n + 2m \leq 4$. We then calculate the magnetic field gradients created by each term in the spherical cell and solve numerically the resulting system of coupled differential equations. We find that the significance of higher-order terms grows very quickly, so we are not able to follow the evolution of the magnetization for a long time. Nevertheless, the model does account for several features of our data. The frequency of phase oscillations predicted by the higher-order model, as determined from the time of the first zero crossing, is in good agreement with measurements, as shown in Fig. 4 with squares. The model also gives the correct sign for the asymmetry observed in the envelope of the SQUID signals. Because of rapid growth of higher-order field gradients we could not obtain a quantitative prediction for τ or the transverse relaxation time T_2^*. Experimentally we find that T_2^* ranges from 50 to 250 sec for g from 12 to 80 μG/cm. We found that $1/T_2^*$ approximately scales with g, resulting in a roughly constant factor of spectral narrowing. Relaxation of the steady-state gradients due to diffusion may play a role in determining T_2^*. In the absence of applied gradients we obtained T_2^* over 800 sec.

We also performed a numerical simulation of the magnetization evolution. Following [13] we calculate the dipolar magnetic interactions in Fourier space and run the numerical model on a grid of 64^3 points. We find that while the numerical model reproduces well all qualitative trends of the data, the edge effects are too large to provide a quantitative prediction for the decay of the phase oscillations in small tip angle data. Quantitative explanation of these effects will require development of new techniques for modeling the behavior of this nonlinear self-interacting system.

In conclusion, we have performed the first detailed study of long-range dipolar interactions by direct measurements of the evolution of magnetization gradients. We find a rich set of features which are generally in good quantitative agreement with simple models. For large tip angles the dipolar effects lead to an exponential gain in sensitivity to magnetic field gradients, while for small tip angles they lead to a lengthening of the transverse spin relaxation time. These effects can be used to enhance the sensitivity in measurements of the magnetic field gradients and average fields, respectively.

This work was supported by NSF, DOE, Packard Foundation, and Princeton University.

[1] J. Jeener, Phys. Rev. Lett. **82**, 1772 (1999).
[2] Y.-Y. Lin, N. Lisitza, S. Ahn, and W. S. Warren, Science **290**, 118 (2000).
[3] B. Villard and P. J. Nacher, Physica (Amsterdam) **284B**, 180 (2000).
[4] K. L. Sauer, F. Marion, P.-J. Nacher, and G. Tastevin, Phys. Rev. B **63**, 184427 (2001).
[5] P. J. Nacher, N. Piegay, F. Marion, and G. Tastevin, J. Low Temp. Phys. **126**, 145 (2002).
[6] J. Jeener, J. Chem. Phys. **116**, 8439 (2002).
[7] M. V. Romalis and M. P. Ledbetter, Phys. Rev. Lett. **87**, 067601 (2001).
[8] S. Giovanazzi, A. Görlitz, and T. Pfau, Phys. Rev. Lett. **89**, 130401 (2002).
[9] B. Driehuys *et al.*, Appl. Phys. Lett. **69**, 1668 (1996).
[10] Tristan Technologies, Inc., 6185 Cornerstone Court East, Suite 106, San Diego, CA 92121.
[11] J. Naghizadeh and S. A. Rice, J. Chem. Phys. **36**, 2710 (1962)
[12] D. Candela, M. E. Hayden, and P. J. Nacher, Phys. Rev. Lett. **73**, 2587 (1994).
[13] T. Enss, S. Ahn, and W. S. Warren, Chem. Phys. Lett. **305**, 101 (1999).